
Article

Not peer-reviewed version

Evaluation of Corrosion Resistance of 904L Composite Plate in High Temperature and High Pressure Gas Field Environment

Shuai Wang ^{*} , Ping Mei , Lijing Chang , Chao Wu , Shaoyun Chen , Qingguo Chen , Guangshan Li

Posted Date: 22 August 2024

doi: 10.20944/preprints202408.1622.v1

Keywords: 904L; composite plate; pressure vessel; pitting corrosion; stress corrosion cracking



Preprints.org is a free multidiscipline platform providing preprint service that is dedicated to making early versions of research outputs permanently available and citable. Preprints posted at Preprints.org appear in Web of Science, Crossref, Google Scholar, Scilit, Europe PMC.

Copyright: This is an open access article distributed under the Creative Commons Attribution License which permits unrestricted use, distribution, and reproduction in any medium, provided the original work is properly cited.

Disclaimer/Publisher's Note: The statements, opinions, and data contained in all publications are solely those of the individual author(s) and contributor(s) and not of MDPI and/or the editor(s). MDPI and/or the editor(s) disclaim responsibility for any injury to people or property resulting from any ideas, methods, instructions, or products referred to in the content.

Article

Evaluation of Corrosion Resistance of 904L Composite Plate in High Temperature and High Pressure Gas Field Environment

Shuai Wang ^{1,2,*}, Ping Mei ¹, Lijing Chang ³, Chao Wu ⁴, Shaoyun Chen ⁴, Qingguo Chen ⁴ and Guangshan Li ^{1,2}

¹ College Of Chemistry&Environmental Engineering, Yangtze University, Jingzhou, Hubei, 434023, China

² Tubular Goods Research Institute, China National Petroleum Corporation & State Key Laboratory for Performance and Structure Safety of Petroleum Tubular Goods and Equipment Materials, Xi'an, Shaanxi 710065, China

³ Changqing Oilfield Company, PetroChina, Xi'an 710000, China

⁴ Tarim Oilfield Company, PetroChina, Korla 841000, China

* Correspondence: 574916060@qq.com; Tel.: +86-187-0926-8798

Abstract: In order to study the corrosion resistance of 904L composite plate pressure vessel under high temperature and high pressure gas field environment, the pitting corrosion and stress corrosion cracking resistance of 904L composite plate body and weld material were compared with those of 2205 composite plate and 825 composite plate, which have been used in high temperature and high pressure gas field environment. The results showed that the pitting resistance of 904L composite plate was lower than that of 825 composite plate and higher than that of 2205 solid solution pure material plate and 2205 composite plate. The corrosion resistance of welds on 904L composite plate with different materials was very different. The corrosion rate of 904L composite plate body, welding seam and surfacing welding were all slight corrosion, and the sensitivity of chloride stress corrosion cracking was low in the simulation of the corrosion environment of high temperature and high pressure gas field. 904L composite plate met the requirements of corrosion resistance of pressure vessel material in high temperature and high pressure gas field environment.

Keywords: 904L; composite plate; pressure vessel; pitting corrosion; stress corrosion cracking

1. Introduction

High temperature and high pressure gas fields face high temperature, high pressure, high salinity, high chlorine and other harsh conditions [1,2], in order to cope with the complex corrosion environment, while taking into account the economy, the current global high temperature and high pressure gas field pressure vessel material mainly uses carbon steel + corrosion resistant alloy composite plate. The commonly used on-site applications include carbon steel+316L composite plate, carbon steel+2205 composite plate, and carbon steel+825 composite plate [3,4].

Through the opening of a high temperature and high pressure gas field pressure vessel over the years, it was found that there are serious pitting problems in the coating of 316L composite plate pressure vessel, indicating that 316L composite plate has a high corrosion risk under high-temperature and high-pressure gas field operating conditions. 2205 pure material pipeline in the high temperature and high pressure gas field in the process of use did not occur obvious corrosion, but due to the carbon steel base and 2205 stainless steel lining heat treatment process is significantly different, resulting in stainless steel lining prone to produce harmful precipitates, some 2205 composite plate pressure vessels in the use of the weld and heat affected zone pitting problems. 825 composite plate pressure vessel in operation after the opening of the can inspection found that its internal surface no pitting occurred, therefore, 825 composite plate can meet the high temperature and high pressure gas field environment on the pressure vessel material corrosion resistance

requirements, but its production and manufacturing costs are high. Therefore, it is necessary to carry out the test and evaluation of new materials with both corrosion resistance and economy.

904L is a highly alloyed super austenitic stainless steel with a very low carbon content, 904L has been standardized in many countries and has been approved for use in the manufacture of pressure vessels. 904L alloy, like other commonly used Cr-Ni austenitic steels, has good resistance to point corrosion, intergranular corrosion and crevice corrosion, high resistance to stress corrosion cracking, good workability and weldability. At present, the production technology of 904L composite plate is more mature, and has been used for petroleum and petrochemical storage, sulfuric acid storage and transportation equipment [5-10]. In terms of price, taking the thickness of 16mm+4mm plate as an example, compared with 825L+Q345R composite plate, the price of 904L+Q345R composite plate is about 40% lower. For the corrosion resistance of 904L stainless steel, predecessors have carried out some relevant studies.

Wang et al. studied the grain boundary sensitization behavior of 904L high nickel austenitic stainless steel using an electron probe. After sensitizing at 650°C for different time periods, 904L was corroded at 1mol/L HCl for 7 days. The results show that there is an obvious 3μm wide corrosion sensitive zone around the grain boundary. The results of EPMA analysis show that there is no obvious segregation near the grain boundaries, and the analysis of transmission electron microscopy shows that there are σ phases precipitated along the grain boundaries, which leads to the discontinuity of 904L grain boundary passivation film and grain boundary sensitization [11].

Khey Sherief A. Al et al. investigated the corrosion behavior of 904L stainless steel in lithium bromide solution. The results showed that the uniform corrosion rate and pitting susceptibility of 904L increased with the increase of lithium bromide concentration and temperature, and the rate of uniform corrosion and pitting was decreased by increasing the pH value of the solution [12].

Wang Quanzhu et al. investigated the corrosion behavior of 904L+ 14Cr1MoR(H) and 904L+Q345R stainless steel composite plates used in CNOOC Huizhou Phase II coal gasification and hydrogen production combined unit after explosive composite and heat treatment. The results showed that the heat treatment system had a great impact on the corrosion performance of 904L. The corrosion resistance of 904L decreased. According to ASTMG150 method, point corrosion experiment was carried out to test critical point corrosion (CPT), 904L+14Cr1MoR (H) and 904L+Q345R two kinds of composite plate critical point corrosion temperature $CPT \geq 40^\circ C$. According to GB/T4334 E method, no intergranular corrosion cracks were detected [13].

Aiming at the problem that 904L+14Cr1MoR(H) composite plate needs to undergo stress relief heat treatment after explosive welding, Zhang Baoqi et al conducted a series of heat treatment tests after explosive composite, and obtained the best heat treatment process through tensile, bending, impact, shear and other mechanical properties tests and laminar corrosion resistance tests. The results show that: after 620~690°C heat treatment, 904L has grain boundary coarsening, carbide precipitation phenomenon in the grain boundary, but the degree is different, but the intergranular corrosion test is qualified. According to the influence of various heat treatment systems on the mechanical properties and corrosion resistance of the material and the thickness of the equipment composite plate body, the final heat treatment process is selected as $(690 \pm 14)^\circ C$, 180min holding time (selected according to the actual thickness), and the comprehensive performance is the best, and its mechanical properties and corrosion resistance can fully meet the design requirements [14].

At present, there is no application case of 904L composite plate in pressure vessel of oil and gas field treatment station, so it is necessary to carry out corrosion resistance evaluation of 904L composite plate in simulated high temperature and high pressure gas field environment, and compare it with 2205 composite plate and 825 composite plate with mature application experience, so as to provide reference for the next step of pressure vessel material selection of high temperature and high pressure gas field.

2. Experiment

2.1. Experimental Materials

Considering the effect of explosive welding of 904L composite plate and heat treatment process on the corrosion resistance of stainless steel in the manufacturing process of composite plate container, the plate with the same heat treatment state as the composite plate pressure vessel was used as the test material, and the welding manufacturing process of different parts of the composite plate pressure vessel was taken into account. Five kinds of materials, including 904L pure material, Q345R+904L composite plate body, Q345R+904L composite plate weld (E385 welding material), Q345R+904L composite plate weld (625 welding material), Q345R+E385 surfacing, were used for evaluation. And compared with the corrosion resistance of Q345R+2205 composite plate, 2205 pure material, Q345R+825 composite plate, the specific test material is as follows:

A total of 8 materials were selected for this test: One is 904L pure material (solid solution state), the second is Q345R+904L composite plate body (the same heat treatment state as the composite plate pressure vessel, simulating the pressure vessel shell base material), the third is Q345R+904L composite plate weld (E385 welding material, the same heat treatment state as the composite plate pressure vessel, simulating the butt weld of the container barrel), The fourth is Q345R+904L composite plate weld (625 welding material, the same heat treatment state with the composite plate pressure vessel, simulating the butt weld of the container cylinder), the fifth is Q345R+E385 surfacing (the same heat treatment state with the composite plate pressure vessel, simulating the surfacing parts of the container seal), the sixth is the Q345R+2205 composite plate body (the same heat treatment state as the composite plate pressure vessel), the seventh is 2205 duplex stainless steel pure material (solid solution state), the eighth is the Q345R+825 composite plate (the same heat treatment state as the composite plate pressure vessel), respectively marked as 1#~8# sample. The chemical composition, metallographic structure and mechanical properties of the 8 kinds of materials have been tested qualified, and the heat treatment parameters of the composite plate and weld are shown in Table 1.

Table 1. Heat treatment parameters of composite plate and weld.

Composite plate material	Heat treatment parameters after explosive composite	Heat treatment parameters after welding
904L+Q345R	1010°C/10 ~ 20min, air cooling to ≤400°C after air cooling	580°C/2h, furnace cooling to ≤400°C after air cooling
825+Q345R	940°C/20 ~ 30min, air cooling to ≤400°C after air cooling	580°C/2h, furnace cooling to ≤400°C after air cooling
2205+Q345R	1050°C/10 ~ 20min air cooling to ≤400°C after air cooling	580°C/2h, furnace cooling to ≤400°C after air cooling

2.2. Experimental Methods

2.2.1. Electrochemical Test

Electrochemical samples were taken from 1#~8# samples respectively, and the progressive action potential polarization curves were measured by C235 electrochemical workstation. A three-electrode system was adopted in the test device, namely, the working electrode (sample), the reference electrode Ag/AgCl and the auxiliary electrode Pt (platinum sheet). The platinum sheet area was 1cm². The test solution was simulated gas field water, the chloride ion concentration was 160000mg/L, the oxygen was removed and the test temperature was 80°C. In order to eliminate the interference of dissolved O₂ on the test results, 0.5h high purity N₂ (99.99%) was injected into the solution before the test, and then 30min CO₂ was injected into the solution to start the test. In order to ensure that CO₂ in the solution was always saturated, the test was started and CO₂ was always kept in the test process.

2.2.2. Iron Trichloride Pitting Test

According to ASTM G48-11(2020) standard, method A (6% ferric chloride solution) was selected to conduct corrosion test on 1#~8# samples at 50°C, and the test time for each sample was 72h. Before and after the test, the sample was measured and weighed and the corrosion rate was calculated.

2.2.3. Weight Loss Test of High Temperature Autoclave

According to ASTM G111-21a standard, corrosion simulation tests were conducted on 1#~8# samples using high temperature autoclave. The test temperature was 80°C, the chloride ion concentration was 160000mg/L, the CO₂ partial pressure was 1.2MPa, the total pressure was 10MPa, there were 3 samples in each group, and the test cycle in each group was 336h.

After the corrosion test, the kettle was removed after cooling and pressure release, and the hanging plates were taken out. The corrosion morphology and product composition on the surface of the hanging plates were analyzed by scanning electron microscope and energy spectrum analysis system. The corrosion products on the surface of the hanging plates were removed by a solution composed of 0.1L hydrochloric acid (analytical pure), 7g hexamethylenetetramine (analytical pure) and 1L deionized water. According to equation (1), the uniform corrosion rate was calculated:

$$V = \Delta m \times 76 \times 10^6 / (\rho t S) \quad (1)$$

where: Δm -- weightlessness of the hanging piece, g; ρ -- specific gravity of the material, g/cm³; t -- test time, h; S -- surface area, mm²; V -- average corrosion rate, mm/a.

Grade the resulting corrosion rate according to NACE RP 0775, as shown in Table 2.

Table 2. Classification of corrosion rates.

Degree of corrosion	Uniform corrosion rate mm/a	Maximum pitting rate mm/a
Light	< 0.025	< 0.13
moderate	0.025-0.12	0.13-0.20
Severe	0.12-0.25	0.21-0.38
Extremely severe	> 0.25	> 0.38

2.2.4. Chloride Stress Corrosion Cracking Test

According to GB/T 15970.1-2018 standard, CORTEST tensile rate tester equipped with high temperature autoclave was used to perform slow strain rate tensile test on 1#~8# samples. The sample was processed into the plate-like sample as shown in Figure 1. Before the test, the sample was polished step by step with 240#, 400#, 600#, 800# and 1000# sandpaper in turn. The surface of the test piece was cleaned with acetone, removed oil, dry with cold air and weighed, and the actual size of the test piece was measured with vernier caliper. The sample was connected to the fixture with a pin of the same material, and an insulating sleeve was installed between the pin and the fixture to prevent the galvanic corrosion of the sample. The test solution was simulated gas field water, the chloride ion concentration was 160000mg/L, the test temperature was 80°C, the CO₂ partial pressure was 1.2MPa, the total pressure was 10MPa. Before the test, the solution was deoxygenated for no less than 20h, and then the test gas was injected into the solution for at least 1 h to saturate the solution, and then heated up to the required temperature of the test. When the temperature was stable, the test gas was increased to the required partial pressure of the test, and then pressurized with nitrogen to the total pressure of 10 MPa. The test was started and stopped after the test broke.

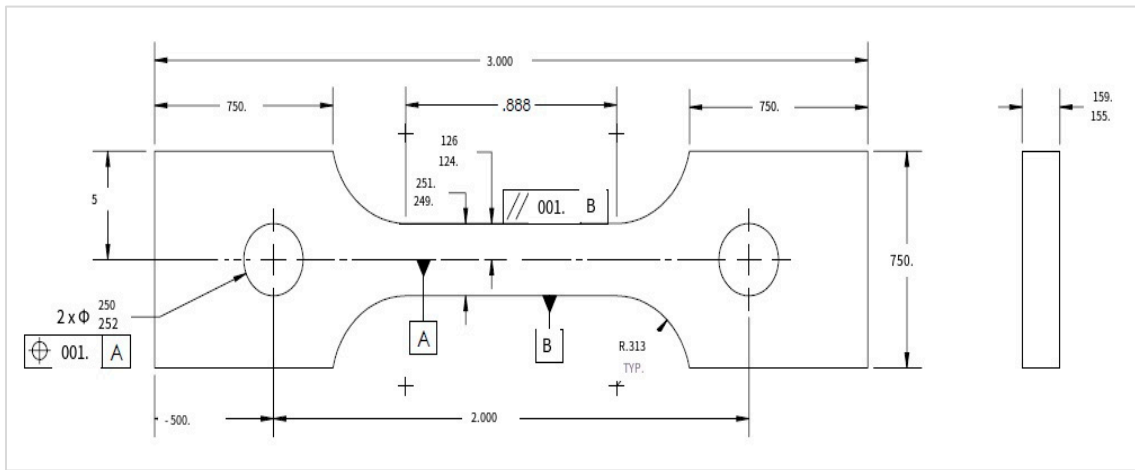


Figure 1. Size of slow strain rate tensile sample (in).

The stress corrosion cracking sensitivity of a material in a certain environment is generally assessed by the stress corrosion sensitivity index I_{SCC} , as shown in equation (2):

$$I_{SCC} = (I_i - I_c) / I_i \times 100\% \quad (2)$$

where, I_{SCC} - stress corrosion sensitivity index;

- I_i -- test parameters in inert medium;
- I_c - Test parameters in corrosive media;

To evaluate the sensitivity index of stress corrosion cracking I_{SCC} , commonly used tensile strength, elongation after fracture and other indicators, the general evaluation method to measure the sensitivity of stress corrosion cracking is shown in Table 3.

Table 3. General evaluation methods for stress corrosion cracking sensitivity.

Stress corrosion sensitivity coefficient	Stress corrosion sensitivity
> 35%	Have a significant tendency to stress corrosion
25% ~ 35%	Some tendency to stress corrosion
Less than 25%	No significant tendency to stress corrosion

3. Results

3.1. Pitting Resistance

Figure 2 shows the potentiodynamic polarization curve of 8 kinds of materials. As can be seen from Figure 2, the pitting and breaking potential of 6# sample (625 weld) is the highest, followed by 8# sample (825 composite plate). It can be seen that the pitting resistance of 625 and 825 materials is stronger than other materials. Compared with the 1# sample (904L pure material), the pitting resistance of the 3# sample (904L composite plate) has little difference; Compared with the 2# (2205 pure material) sample, the 3# sample (904L composite plate) pitting rupture potential is higher and the critical passive current density is smaller, indicating that the pitting resistance of the 904L composite plate material is stronger than that of the 2205 pure material. The pitting rupture potential of the 4# sample (E385 weld) and the 5# sample (E385 surfacing) is slightly lower than that of the 2205 pure material, but the critical passive current density is less than that of 2205 pure material. From a comprehensive analysis, the pitting resistance of 904L composite plate weld (E385) and surfacing (E385) specimens is similar to that of 2205 pure material, and the results are shown in Table 4.

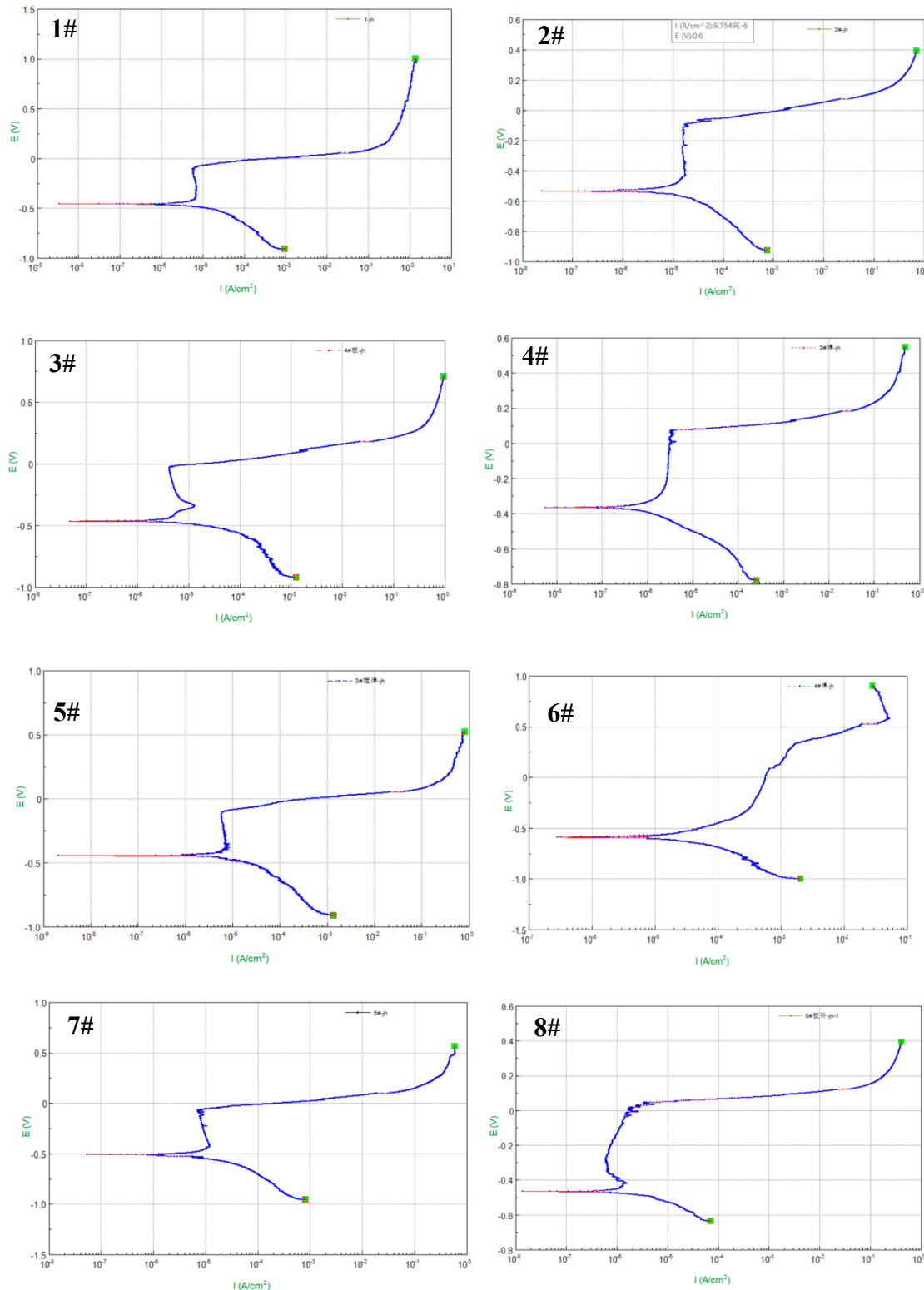


Figure 2. Potentiodynamic polarization curve of the specimen.

Table 4. Electrochemical test results.

No.	Material	Pitting break potential E_b (V)	Critical passive current density i_p ($\mu\text{A}/\text{cm}^2$)
1 #	904L pure wood	0.111	7.08
2 #	2205 Pure wood	0.098	16.00
3 #	904L composite plate	0.029	5.29

4 #	E385 Weld	0.102	5.65
5 #	E385 surfacing	0.112	6.72
6 #	625 Weld	0.259	3.70
7 #	2205 composite plate	0.072	9.09
8 #	825 composite plate	0.044	0.86

The results of iron trichloride pitting test show that 825 composite plate has the lowest weight loss and the lowest corrosion rate per unit area, followed by 625 weld; The corrosion rate of 904L pure material and 904L composite plate is lower than that of 2205 pure material and 2205 composite plate, but the corrosion rate of E385 weld and E385 surfacing welding is higher than that of 2205 pure material and 2205 composite plate. The average corrosion rate from large to small is E385 surfacing > E385 weld > 2205 composite plate > 2205 pure material > 904L composite plate > 904L pure material > 625 weld > 825 composite plate, as shown in Table 5.

Table 5. Results of ferric trichloride pitting test.

No.	Material	Weight before sample(g)	Weight after sample(g)	Weight loss(g)	Area(cm ²)	Mass loss(g/cm ²)
1#	904L pure wood	15.9671	15.8196	0.1475	14.9688	9.85 E-03
2#	2205 Pure material	14.3944	14.1123	0.2821	15.0859	1.87E-02
3#	904L composite plate	12.9069	12.6761	0.2308	14.8641	1.55 E-02
4#	E385 Weld	11.9554	11.3134	0.642	14.5075	4.43 E-02
5#	E385 surfacing	11.1224	10.2061	0.9163	14.2994	6.41 E-02
6#	625 Weld	14.6628	14.6323	0.0305	14.8054	2.06 E-03
7#	2205 composite plate	14.0658	13.5457	0.5201	14.7791	3.52 E-02
8#	825 composite plate	13.4271	13.4089	0.0182	14.8457	1.23 E-03

3.2. Corrosion Resistance under Simulated Working Conditions

As can be seen from the corrosion rate calculation results, the uniform corrosion rate of the 8 materials in the simulated high-temperature and high-pressure gas field environment is small, all of them are mild, as shown in Table 6. This indicates that the 8 materials all have strong ability to resist uniform corrosion under the environment of high temperature and high pressure gas field. Taking the 904L composite plate body as an example, the corrosion products on the surface of the hanging sheet are less after corrosion simulation test, the surface of the hanging sheet is bright after cleaning and removing the film, and no obvious pitting corrosion is seen by the naked eye. After magnification 100 times by ultra depth of field microscope, it was found that the surface morphology of the hanging plate was mainly scratches polished during sample processing, and the corrosion marks were not obvious, as shown in Figures 3 and 4.

Table 6. Corrosion test results.

No.	Sample number	Weight before soaking (g)	Length (mm)	Width (mm)	Thickness (mm)	Weight after soaking (g)	Weightlessness (g)	Uniform corrosion rate (mm/a)	Average (mm/a)
	11	8.5951	39.9	9.83	3.02	8.5949	0.0002	0.0006	
1#	12	8.3942	39.94	9.89	2.94	8.3939	0.0003	0.0009	0.0006
	13	8.415	39.94	9.9	2.92	8.4149	0.0001	0.0003	
	21	8.3305	39.84	9.91	2.97	8.3303	0.0002	0.0006	
2#	22	8.3211	39.84	9.82	2.99	8.3208	0.0003	0.0009	0.0008
	23	8.1886	39.9	9.91	2.92	8.1883	0.0003	0.0009	
3#	31	8.6541	39.69	9.97	3.00	8.654	0.0001	0.0003	0.0003
	32	8.6359	39.7	9.95	2.98	8.6358	0.0001	0.0003	

33	8.6296	39.64	9.98	3.02	8.6295	0.0001	0.0003	
3A	7.9332	39.76	9.88	2.79	7.933	0.0002	0.0006	
4#	3B	8.0547	39.75	9.88	2.82	8.0541	0.0006	0.0018
	3C	8.2399	39.74	9.92	2.88	8.2398	0.0001	0.0003
	3D	8.531	40.15	9.99	2.94	8.5309	0.0001	0.0003
5#	3E	8.1471	40.21	10.05	2.77	8.147	0.0001	0.0003
	3F	7.9005	40.12	10.08	2.72	7.9005	0	0
	4A	8.804	39.64	10	2.96	8.8036	0.0004	0.0011
6#	4B	8.7926	39.73	9.99	2.97	8.7923	0.0003	0.0009
	4C	8.9265	39.72	9.98	2.98	8.9256	0.0009	0.0026
	51	8.2491	39.88	9.92	2.92	8.2483	0.0008	0.0025
7#	52	7.9776	39.87	9.83	2.90	7.9775	0.0001	0.0003
	53	8.1173	39.85	9.89	2.89	8.117	0.0003	0.0009
	61	8.6737	39.71	9.96	2.98	8.6731	0.0006	0.0018
8#	62	8.5877	39.68	9.95	2.93	8.5876	0.0001	0.0003
	63	8.3706	39.72	9.95	2.87	8.3705	0.0001	0.0003

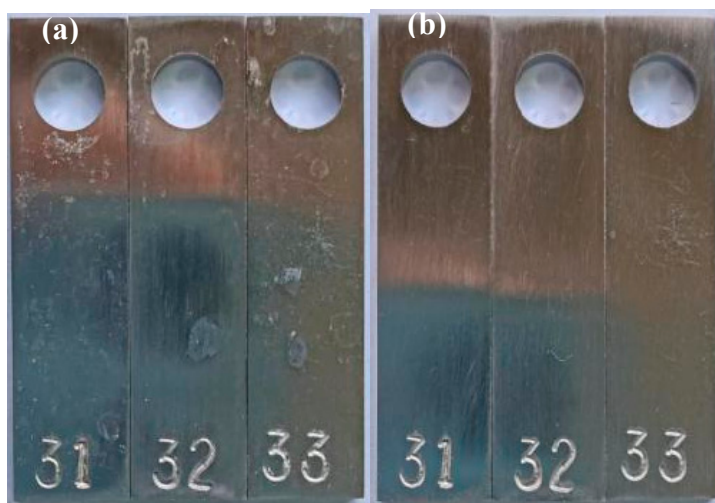


Figure 3. The macro morphology of 3# sample (904L composite plate) before and after film removal
(a) before removing the membrane; (b) after removing the membrane.



Figure 4. Micro-morphology after film removal (100X).

3.3. Resistance to Chloride Stress Corrosion Cracking

Table 7 shows the slow strain rate tensile test results of 8 materials such as 904L composite plate. It can be seen from Table 7 that the stress corrosion cracking sensitivity coefficients of 8 materials are all lower than 25%, indicating that their stress corrosion cracking sensitivity is low under simulated working conditions. According to the test results, the stress corrosion sensitivity coefficient of 825 composite plate and 625 weld material is the lowest, and the stress corrosion sensitivity of 904L composite plate, weld and surfacing material is comparable to that of 2205 plate.

Table 7. Results of slow strain rate tensile test.

No.	Material	Tensile strength			Elongation		
		Corrosion sample (MPa)	Blank sample(MPa)	Change rate(%)	Corrosion sample (%)	Blank sample (%)	Change rate (%)
1#	904L pure wood	524	622	15.76	42.33	52.04	18.66
2#	2205 Pure wood	671	782	14.19	28.49	35.35	19.41
3#	904L composite plate	645	756	14.68	38.00	46.93	19.03
4#	E385 Weld	487	559	12.88	/	/	/
5#	E385 surfacing	489	561	12.83	/	/	/
6#	625 Weld	699	775	9.81	/	/	/
7#	2205 composite plate	695	827	15.96	34.65	42.16	17.81
8#	825 composite plate	628	718	12.53	31.68	38.02	16.68

4. Discuss

904L is a super austenitic stainless steel, which has good corrosion resistance, so it is mainly used in harsh corrosion conditions, the current production technology is mature, many steel mills at home and abroad have the production capacity. According to the performance information provided by a composite plate pressure vessel manufacturer, 904L composite plate pressure vessel has been applied in pressure vessels such as acetic anhydride hydration reactors of some petrochemical enterprises, and the application situation is good, but there is no report on the application of 904L composite plate pressure vessel in upstream oil and gas field treatment stations. The following combined with the results of the corrosion resistance evaluation test, from the three aspects of pitting resistance, uniform corrosion and stress corrosion cracking performance, the applicability of the 904L composite plate pressure vessel under the working conditions of high temperature and high pressure gas fields is analyzed.

(1) pitting resistance

When stainless steel is in a chlorine-containing environment, point corrosion will occur at a certain temperature [15–21]. As we all know, the improvement of chromium and molybdenum content helps to enhance the ability of stainless steel to resist local corrosion, chromium, molybdenum and nitrogen on the combined impact of local corrosion resistance is often expressed by pitting resistance equivalent PREN [22], the commonly used formula is as follows:

$$\text{PREN} = \% \text{ chromium} + 3.3 \times \% \text{ molybdenum} + 16 \times \% \text{ nitrogen}$$

Table 8 shows the pitting resistance equivalent comparison between 904L and several common stainless steels in oil fields. As can be seen from Table 3, the PREN value of 904L super austenitic stainless steel is significantly higher than that of 316L, which is also higher than that of 2205 duplex stainless steel.

Table 8. Comparison of pitting resistance equivalent of several stainless steels.

Grades of stainless steels	ASTM	PREN
316L	S31603	26
2205	S31803	33
904L	N08904	34
825	N08825	35

According to the electrochemical test results, the pitting corrosion resistance of 904L pure material and 904L composite plate material is stronger than that of 2205 pure material, and lower than that of 825 composite plate and 625 welding material. The pitting resistance of 904L composite plate's welds and surfacing welding (both E385 welding materials) is lower than that of 904L pure material and 904L composite plate, and the pitting resistance of 2205 pure material is close. The results of ferric trichloride pitting test show that the corrosion rate of 904L pure material and 904L composite plate is lower than that of 2205 pure material and 2205 composite plate, but the corrosion

rate of E385 weld and surfacing welding of 904L composite plate is higher than that of 2205 pure material and 2205 composite plate.

(2) Uniform corrosion resistance

According to the weight loss test results of high temperature autoclave, 904L pure material, 904L composite plate, E385 weld, E385 surfacing, 625 weld, 2205 composite plate, 2205 pure material and 825 composite plate all have low corrosion rate under simulated high temperature, high pressure and high Cl^- environment. According to the provisions of NACE RP0775, the corrosion rate is graded, and all of them are slight corrosion levels.

(3) Resistance to chloride stress corrosion cracking

According to the slow strain rate tensile test results of 8 kinds of materials under simulated working conditions, the stress corrosion cracking sensitivity coefficients of 904L composite plate, weld and surfacing materials are all lower than 25%, indicating that the stress corrosion cracking sensitivity is low under simulated working conditions. In addition, the stress corrosion cracking sensitivity coefficient of 904L plate is not much different from that of 2205 plate. According to the field application of 2205 material pressure vessel in a high temperature and high pressure gas field for nearly 20 years, the inspection defects of 2205 composite plate pressure vessel over the years are mainly pitting corrosion at the weld, and the number of chloride stress corrosion cracking is very small. And the main reason is that the material of 2205 composite plate is unqualified and there is precipitated phase. Therefore, it is judged that the possibility of chloride stress corrosion cracking of 904L composite plate under the working condition of high temperature and high pressure gas field is low.

5. Conclusion

(1) Electrochemical and ferric chloride pitting test results show that: The pitting resistance of 904L composite plate is not significantly lower than that of 904L pure plate. The pitting resistance of 904L composite plate is lower than that of 825 composite plate and higher than that of solid-solution 2205 pure plate and 2205 composite plate. The pitting resistance of E385 weld and surfacing welding is lower than that of solid-solution 2205 pure plate and 2205 composite plate. The pitting resistance of the 625 weld is higher than that of the solid-solution 2205 pure material plate and 2205 composite plate.

(2) The weight loss test results of high temperature autoclave show that the corrosion rate of 904L composite plate body, weld and surfacing welding all belong to slight corrosion level under the corrosion environment simulating high temperature and high pressure gas field.

(3) The slow strain rate tensile test results show that: in the simulated high-temperature and high-pressure gas field corrosion environment, 904L composite plate body, weld and surfacing welding chloride stress corrosion cracking sensitivity is low.

(4) 904L composite plate meets the requirements of pressure vessel material corrosion resistance in high temperature and high pressure gas field environment, and has a good application prospect in processing equipment in oil and gas field station. Field tests can be carried out from small pressure vessels.

Author Contributions: Methodology, S.W. and P.M.; Validation, L.C. and C.W.; investigation, S.C.; writing—original draft preparation, Q.C.; writing—review and editing, G.L. All authors have read and agreed to the published version of the manuscript.

Funding: This research was funded by China's national key R&D plan "Research on Safety Assessment and Risk Assessment and Early Warning of Crude Oil and Natural Gas Storage Tanks, Auxiliary Pipelines and Auxiliary Facilities" (2017YFC0805804).

Data Availability Statement: The data used to support the findings of this study are available from the corresponding author upon request.

Acknowledgments: Thanks to Tubular Goods Research Institute, China National Petroleum Corporation, from Xi'an, China and Tarim Oilfield Company, petrochina, from Korla, China, for their cooperation and enabling the experimental equipment and technical guidance for the implementation of our research.

Conflicts of Interest: The authors declare no conflict of interest.

References

1. Zheng, J.; et al. Establishment and application of temperature-pressure coupling model for opening and closing wells in HTHP gas wells. *Energy Exploration & Exploitation*. 2024, 42, 1359-1385.
2. Ji, N.; et al. Collapse failure analysis of S13Cr-110 tubing in a high-pressure and high-temperature gas well. *Engineering Failure Analysis*. 2023, 148.
3. Li, L.; Chen, Q.; Fang, Y.; Li, X.; Luo, J.; Song, C.; Wang, S. Failure analysis of 2205 duplex stainless steel connecting pipe for composite plate pressure vessel in a high pressure gas field. *International Journal of Pressure Vessels and Piping*. 2023, 202.
4. Wang, Z.; Kang, S.; Xu, M.; Cheng, Y.; Dong, M. Effect of Heat Treatment on Microstructure and Properties of Clad Plates 316L/Q370qE. *Materials*. 2019, 12, 1556-1556.
5. Ceyhun KOSE. Effect of post-weld heat treatment on microstructure, crystallography, and mechanical properties of laser beam welded AISI 904L super austenitic stainless steel. *Engineering Failure Analysis*. 2024, 158, 108025-.
6. Xu, D.; Zhang, X.; He, X. Mechanism and evaluation method of stress corrosion susceptibility of 904L stainless steel with optimized structure in seawater. *Corrosion Science*. 2024, 229, 111865-.
7. S. A. Y. K. A. G., et al. New Insights on the Corrosion-Erosion Behavior of 904L Stainless Steel in Phosphoric Acid Containing Impurities. *Journal of Bio- and Triboro-Corrosion*, 2024, 10, 1.
8. Bai, L.; Peng, W.; Li, W.; Shi, X. Effect of titanium element on high temperature chlorine corrosion properties of 904 L alloy. *Corrosion Science*. 2023, 211.
9. Mändl, S.; Manova, D. Comparison of Nitriding Behavior for Austenitic Stainless Steel 316Ti and Super Austenitic Stainless Steel 904L. *Metals*. 2024, 14, 659-.
10. Prabu, S. S.; M. S. M. N. B., et al. Microstructure and mechanical assessment of Inconel 625 and AISI 904L dissimilar joints using high-density welding technique for pressure vessels. *International Journal of Pressure Vessels and Piping*. 2024, 209, 105191-.
11. Wang, J.; Shi, W.; Xiang, S.; B. R. G. Study of the corrosion behaviour of sensitized 904L austenitic stainless steel in Cl- solution. *Corrosion Science* prepublish. 2021, 109234-.
12. Al A S K, El A A E M, El A S S R. Electrochemical Investigations on the Corrosion Behavior of 904L Stainless Steel in LiBr Solutions. *Journal of Materials Engineering and Performance*. 2023, 32, 163-9173.
13. Wang, Q.; et al. Corrosion Performance Study of 904L (N08904) Stainless Steel Composite Plate Material Development and Application. 2017, 32, 53-58.
14. Zhang, B.; et al. Study on Heat Treatment Process of 904L+14Cr1MoR (H) Composite Plate Corrosion and Protection in Petrochemical Industry. 2015, 32, 12-17.
15. Liu, X.; Zhu, X.; Liu, Z. Role of Cl/F Ions Concentration, pH and Temperature on Pitting Corrosion Behavior of 2507 Duplex Stainless Steel. *Journal of Physics: Conference Series*. 2024, 2731, 1.
16. Nuthalapati, S.; Kee, E. K.; Ismail, C. M.; et al. Comparative study of corrosion behaviour and microstructural analysis of as-received and sensitized SS304 U-bend samples under perlite thermal insulation using chloride drip test. *Engineering Failure Analysis*. 2024, 159, 108054-.
17. Yoo, S. J.; Chung, T. N.; Lee, H. Y., et al. Effect of Sulfide and Chloride Ions on Pitting Corrosion of Type 316 Austenitic Stainless Steel in Groundwater Conditions Using Response Surface Methodology. *Materials*. 2023, 17, 1.
18. Geng, Y.; Liu, Z.; Zeng, W.; Feng, Y.; Ding, B. How to Choose the Suitable Steel of Wellhead, Wellbore, and Downhole Tools for Acid Gas Reinjection Flooding. *Processes*. 2022, 10, 2685-2685.
19. Quynh, L. H.; Ralph, B.; Dirk, B., et al. Corrosion Study on Wellbore Materials for the CO₂ Injection Process. *Processes*. 2021, 9, 15.
20. Souza, D. M. L.; Pereira, E.; Amaral, S. D. B. T., et al. Corrosion Study on Duplex Stainless Steel UNS S31803 Subjected to Solutions Containing Chloride Ions. *Materials*. 2024, 17, 9.
21. Li, B.; Lang, Y.; Chen, H.; Qu, H.; Feng, H.; Sun, X.; Tian, Z. Studies on the Cooperative Influence of Cr and Mo on the Pitting Corrosion Resistance of Super Austenitic Stainless Steels. *Materials*. 2023, 16, 23.
22. Kannan, T.; Murugan, N. Effect of Welding Parameters on Pitting Resistance Equivalent Number of Duplex Stainless Steel Clad Metals. *Indian Welding Journal*. 2006, 39, 8-23.

Disclaimer/Publisher's Note: The statements, opinions and data contained in all publications are solely those of the individual author(s) and contributor(s) and not of MDPI and/or the editor(s). MDPI and/or the editor(s) disclaim responsibility for any injury to people or property resulting from any ideas, methods, instructions or products referred to in the content.